International Journal Of Engineering Research And Development
e- ISSN: 2278-067X, p-ISSN: 2278-800X, www.ijerd.com
Volume 19, Issue 3 (May.-June. 2023), PP. 38-51

Fracture of soda lime glass under impact loading.

Jaroslav Buchar[1], Jan Trnka[1], Radek Řídký [2]
[1] *Institute of Thermomechanics, CAS, Dolejskova 5, 182 00 Prague, Czech Republic,*
e-mail: trnka@it.cas.cz, buchar@it.cas.cz.
[2] *SVS FEM,LtD.,Trnkova 117c, 628 00 Brno, Czech Republic,*
e-mail: rridky@svsfem.cz

ABSTRACT:*A modified method of the dynamic Brazilian test was used to study of fracture of soda – lime glass. This method is based on the Hopkinson pressure bar when the specimen is loaded by the direct impact of a striker. Specimen response to the impact loading is given by the stress pulse monitored in the pressure bar. The main characteristics of these pulses are compared with those obtained using the common dynamic Brazilian test. The use of the high speed camera showed that the qualitative features of the specimen fracture are very similar even if not the same for both used experimental techniques. The Johnson-Holmquist ceramic model (JH2) was used for the numerical simulation of the modified method using LS DYNA software. It was found that the agreement between the computed and the experimental results improved with the increase in the striking velocity.*
Key Words: *Impact loading; Dynamic Brazilian test; Hopkinson pressure bar; Fracture strength; High speed photography; JH2 model; Numerical simulation*.

Date of Submission: 01-06-2023 Date of Acceptance: 12-06-2023

I. INTRODUCTION

The knowledge of the fracture properties of glass play significant role in the planning of their use in many practical application when e.g. glass windows are especially vulnerable to shock and impact loading [1]. Under impact loading conditions, the glass system fails or cracks due to the reflection of the compressive wave from the back free surface as a tensile one and low tensile strength of glass. Therefore, to be evaluated under different loading-rates the tensile strength and tensile failure of brittle materials (ceramics, rocks etc.) Extensive experimental and numerical research has been conducted to understand glass performance during dynamic and static tests. Most of this research [2-6] studied the blast response of various types of glass, while others [7–13] focused on fracture mechanisms in different types of impact.

The measurement of the tensile strength of the glass as well as other brittle materials is very difficult owing to its brittleness, high hardness, and very small strain to failure. These problems may be overcome by the use of indirect tensile test known as the Brazilian test. Its use for the study of the glass fracture behavior was reported in many papers, see e.g. [14, 15] as examples. Even if in this test the strain rates reaches values typical for the impact loading processes the boundary value conditions are different from e.g. direct impact of the tested body.

The present paper is focused on the modification of the dynamic Brazilian test when the glass specimen is loaded by the direct impact of a striker. The aim of the paper consists in the evaluation of the effect of the different loading condition on the fracture characteristics of the soda – lime glass specimens.

II. MATERIAL AND EXPERIMENTAL PROCEDURE

Soda – lime glass was chosen as testing glass material. This material is considered as linear elastic up to the fracture. Its elastic properties are commonly evaluated using the values of the longitudinal and shear wave velocities. The velocities of the longitudinal wave, c_L, and shear wave, c_T, were measured ultrasonically by pulse echo method using Physical Acoustics Corporation μDiSP system. The longitudinal wave velocity was determined with 3.5MHz Aerotech Gamma probe, the shear wave velocity was determined with normal incidence shear wave transducer V154 by Olympus operating at 2.25 MHz. The values of Poisson`s ratio,$\nu$, Young`s modulus and shear modulus, G are given as [16]:

$$\nu = \frac{c_L^2 - 2c_T^2}{2(c_L^2 - c_T^2)} \qquad (1a)$$

$$E = 2\rho c_T^2(1+\nu) \qquad (1b)$$

$$G = \frac{E}{2(1+\nu)} \qquad (1c)$$

The obtained elastic properties of materials used during the experiments are listed in the Table 1.

Table 1: Material properties

Properties	Glass	Tool steel	HDPE
Material density ρ (kg/m^3)	2490	7850	960
Longitudinal wave velocity, c_L, (m/s)	5810	6060	2416
Shear wave velocity, c_T, (m/s)	3440	3150	1010
Elastic modulus, E, (GPa)	72.5	216	2.73
Poisson`s ratio,ν	0.23	0.31	0.39
Shear modulus, G, (GPa)	29.5	77.9	0.98
Bar velocity, $c_0 = \sqrt{\frac{E}{\rho}}$ (m/s)	5395.7	5246	1686.5
Acoustic impedance, Z= ρc_0 , (MPas/m)	13.44	41.18	1.62

The elastic properties of the glass are in very good agreement with compilation of elastic data of soda-lime glass presented in [17].
Specimens in form of cylinders, 14 mm in diameter and 7 mm in thickness were prepared both for the dynamic Brazilian test and direct impact test.
Dynamic Brazilian test was performed using Hopkinson Split Pressure Bar (HSPB) system as schematically shown in the Fig.1.

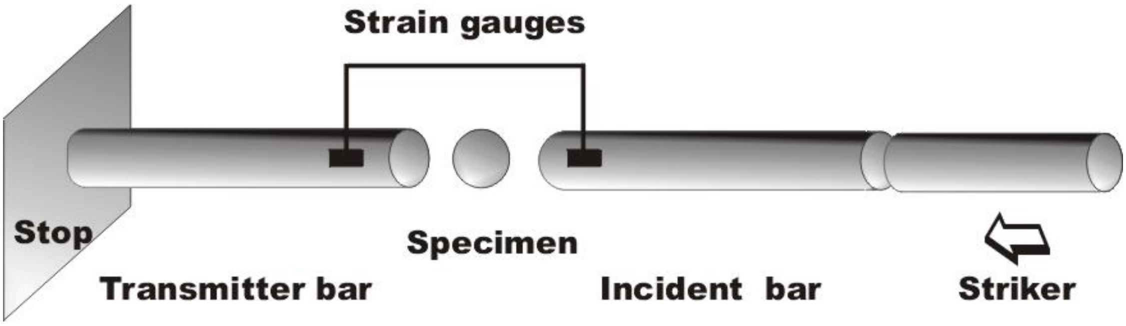

Figure 1: Schematic of the dynamic Brazilian test

This system consists of three main parts. First of all there is a gas gun enabling to accelerate the projectile (striker) to some velocity. Second part is a system two elastic bars (incident and transmitted) and the third part is the data acquisition system. After impact of the striker on the end of the incident bar the compressive stress pulse (incident stress pulse), $\sigma_I(t)$, is developed. After impact of this wave on the interface between the incident bar and specimen some part is reflected back as the reflected stress pulse,σ_R (t) and part is transmitted to the second bar as the stress pulse $\sigma_T(t)$. The evaluation of these stress pulses is based on the assumption of the elastic behavior of the bars during the test. The stress pulses are than calculated using the signals from the strain gauges pasted on the bars:

$$\sigma_I = E_b\varepsilon_I \quad \sigma_R = E_b\varepsilon_R \quad \sigma_T = E_b\varepsilon_T$$

where E_b is the Young`s modulus of the bar, ε_I, ε_R and ε_T are the incident, reflected and transmitted strains, respectively.
The stress pulses enable to calculate the forces at the interface between bar and specimen:

$$P_1(t) = A_b[\sigma_I(t) + \sigma_R(t)]\ ,\ P_2(t) = A_b\sigma_T(t) \qquad (2)$$

Where A_b is the area of the bars.
The evaluation of the results of the dynamic Brazilian test is based on the assumption of the stress equilibrium before the specimen failure, i.e. $P_1 = P_2$. Tensile stress in the center of the glass specimens due to diametric compression is than given by the Eq. (2):

$$\sigma_t = \frac{2A_b\sigma_T(t)}{\pi Dt} \qquad (3)$$

The input and output(transmitter) bars (each 15 mm in diameter and 1000 mm in length) are made from the tool steel. The striker was made from High density polyethylen (HDPE) 15 mm in diameter, 50 mm in length. Main

elastic properties of bars and striker were evaluated using the same experimental technique as used for the glass specimen. Their values are given in the Table 1.
The method shown in the Fig.1 was modified by omitting of the input bar. The specimen is loaded by the direct impact of the striker – see Fig.2. During this test the stress pulse, $\sigma_I(t)$ is recorded.

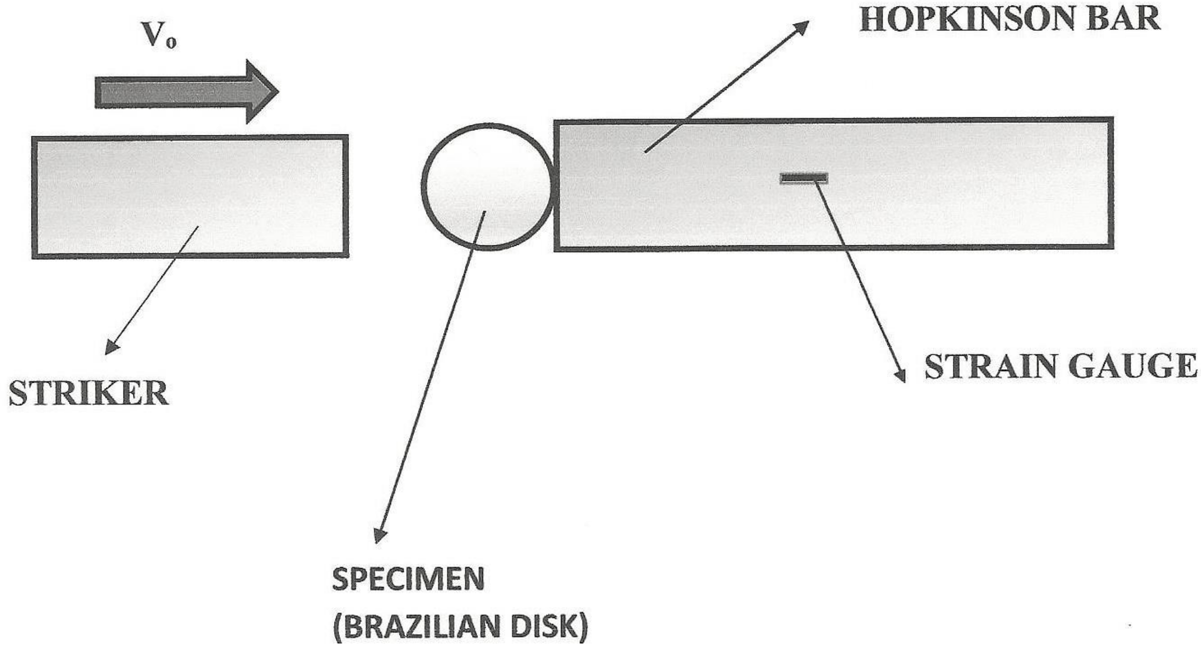

Figure 2: Schematic of a modified dynamic Brazilian test- direct impact

The specimen behaviour during impacts was monitored by high speed photography, using PHOTRON FASTCAM SA-Z type 2100K-M, Frame Rate 210000fps, Shutter Speed 1.00 µs. Resolution 384x160 dpi. with frame rate of 150 000 frames per second.

III. EXPERIMENTAL RESULTS.

The specimens were loaded using the method shown in the Fig.2. The striker impact velocities were: 62, 66, 90, 95 and 100 m/s. The experimentally recorded stress time histories are displayed in the Fig.3. The experimental curves, σ_I (t), can be fitted using the Gaussian model:

$$\sigma_I(t) = \sum_{i=1}^{n} a_i exp\left[-\left(\frac{t-b_i}{c_i}\right)^2\right] \qquad (4)$$

Parameters a_i,b_i,c_i, are given in the Table 2.

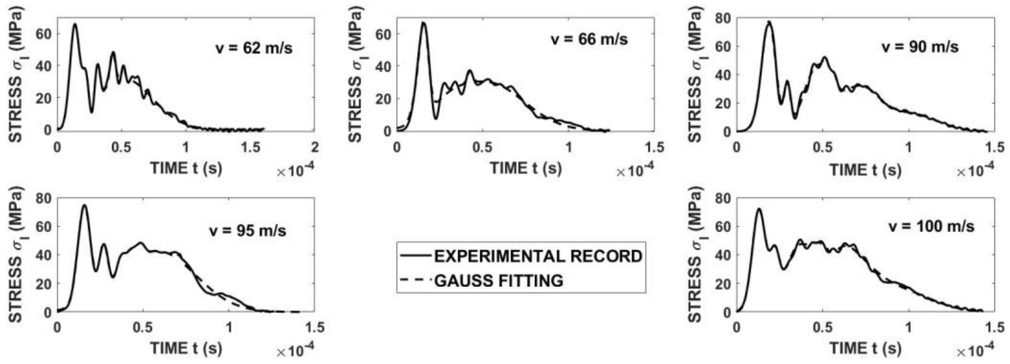

Figure 3: Experimental records of the stress pulses $\boldsymbol{\sigma_I(t)}$

Table 2: Parameters of Eq.(4).(R^2 is correlation coefficients)

Parameters	v = 62 m/s	v = 66 m/s	v = 90 m/s	v = 95 m/s	v = 100 m/s
a_1 (MPa)	64.42367	35.06706	63.42299	50.80419	74.7731
b_1(s)	1.39E-5	1.72E-5	1.82E-5	1.6E-5	1.3E-5
c_1(s)	5.29E-6	3E-6	4.37E-6	4.66E-6	5.45E-6
a_2	21.07128	17.07972	22.22625	-1.6889	8.642562
b_2	4.38E-5	4.23E-5	5.14E-5	4.74E-5	3.66E-5
c_2	2.35E-6	2.87E-6	2.45E-6	4.41E-6	2.04E-6
a_3	30.05139	45.50152	4226635	35.11285	15.92814
b_3	3.16E-5	1.4 E-5	4.57 E-5	2.68 E-5	4.85 E-5
c_3	2.62-6	4.25E-6	6.34E-6	3.67E-6	6.25E-6
a_4	13.00818	42.11121	12.95728	16.65139	-1636.02
b_4	5.15 E-5	5.13 E-5	9.87 E-5	4.27 E-5	5.04 E-5
c_4	175E-6	4.45E-6	2.32E-6	8.21E-6	1.67E-5
a_5	27.13974	17.185	29.55393	-2.57443	30.80875
b_5	2.21 E-5	3.35 E-5	5.62 E-5	5.48 E-5	2.22 E-5
c_5	2.75E-6	3.34E-6	4.07E-6	2.3E-6	3.3E-6
a_6	30.04612	28.36262	23.14653	43.71823	19.8121
b_6	5.64 E-5	5.66 E-5	2.65 E-5	5.98 E-5	9.02 E-5
c_6	2.77 E-5	2.72 E-5	1.35 E-5	2.9 E-5	2.7 E-5
a_7	11.26084	21.691	28.98092	-2.52383	1669.704
b_7	4.02 E-5	2.74 E-5	7.16 E-5	6.21 E-5	5.04 E-5
c_7	4.03E-6	2.63E-6	1.42E-5	1.04E-6	1.71E-5
a_8 (MPa)	0	0	9.484173	22.42602	0
b_8 (s)	0	0	6.34E-05	1.5E-5	0
c_8 (s)	0	0	1.98E-6	5.75E-6	0
R^2	0.9909	0.9911	0.9722	0.9871	0.9969

No damage of the specimen loaded by the striking of the projectile at velocity 62 m/s was observed. The specimen damage starts at the striking velocity 66 m/s. This damage was limited to a relative small area at the contact between the specimen and elastic bar. The development of this damage is illustrated in the Fig.4a.

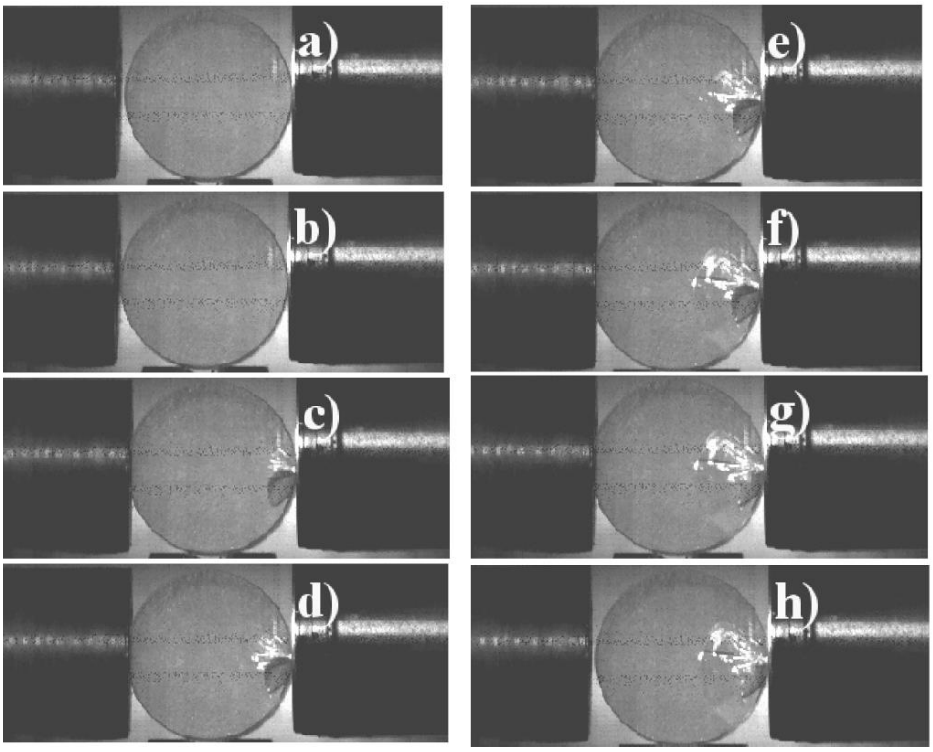

Figure 4a: High speed images of failure process in specimen at different times. Striker velocity was 66 m/s. The images left side represents to the striker-specimen interface and the right part to elastic bar-specimen interface.

The times of corresponding to the single frames are shown in the Fig.4b.

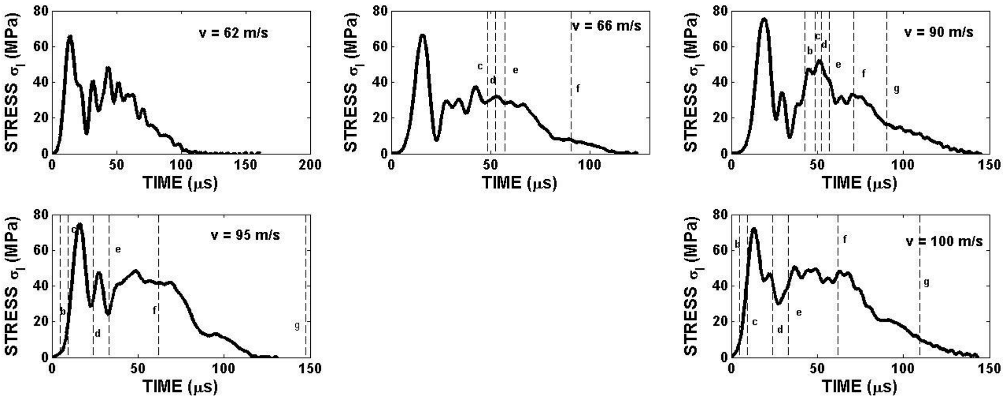

Figure 4b: The times corresponding to the single frames for all tested specimens

First a crack initiated at the contact interface (c). From this crack, many cracks propagated from the surface of the specimen to the centre. The specimen damage starts after the maximum of the stress is reached.

The damage development of the specimen impacted at the velocity 90 m/s is shown in the Fig.5. It is evident that the damage starts again after the maximum of the stress was reached. This damage begins in the form of two wing-like cracks. The two wing-like cracks merged and continued to propagate as a single crack, reaching the far end of the specimen (e).

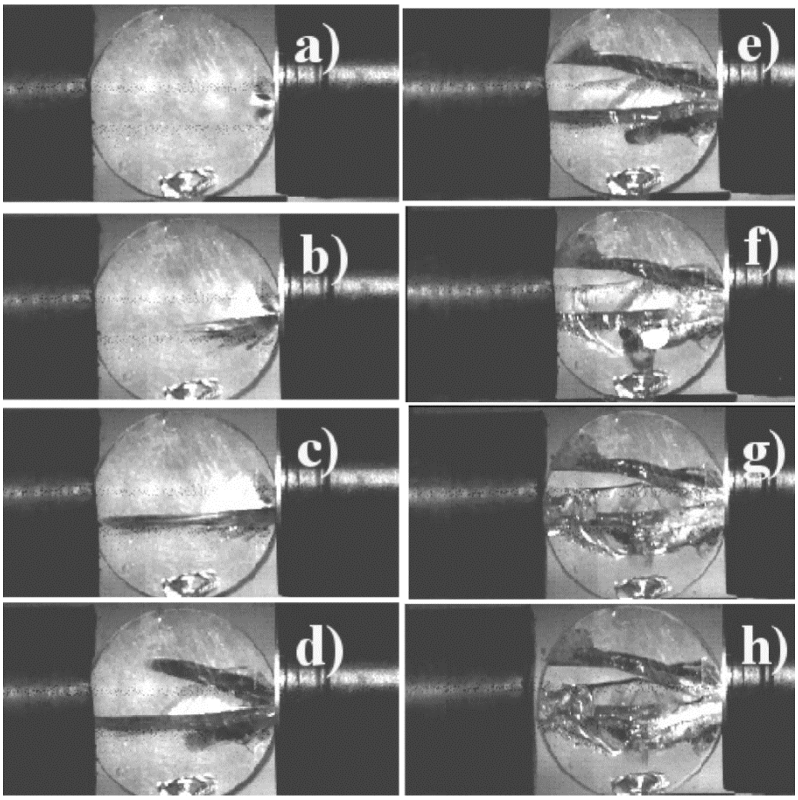

Figure 5: High speed images of failure process in specimen at different times. Striker velocity was 90 m/s

The damage of the specimen growths and specimen splitting occurs. The damage of the specimen observed for the striking velocity 95 m/s is reported in the Fig.6.

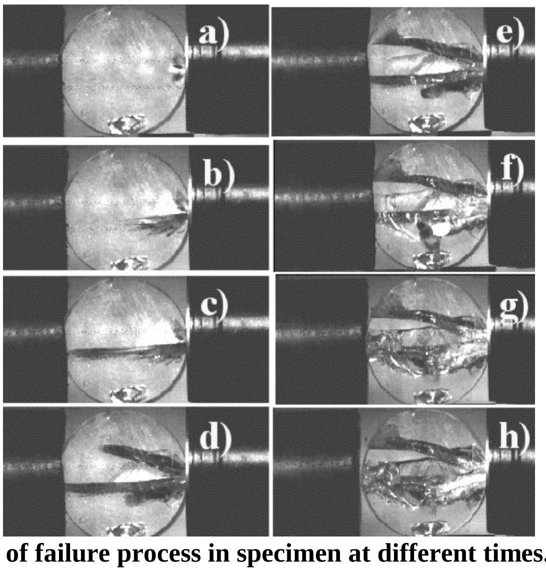

Figure 6: High speed images of failure process in specimen at different times. Striker velocity was 95 m/s

The specimen damage also starts after the stress reached its maximum as it was reported for the previous striking velocities. After the central cracks reached the interface between the striker and the specimen two wing-like cracks started to propagate. Very similar features of the specimen damage can observed at the specimen impacted at the 100 m/s - see Fig.7.

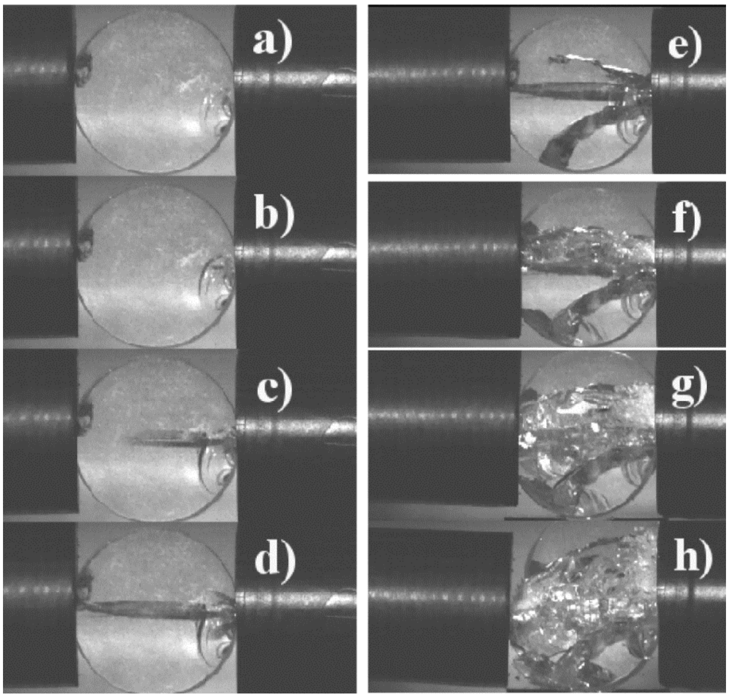

Figure 7: High speed images of failure process in specimen at different times. Striker velocity was 100 m/s

The damage starts when the stress pulse maximum is achieved. It is obvious that the stress pulse maximum σ_{Im} can be considered as a measure of the specimen strength. This maximum increases with the striking velocity as shown in the Fig.8.

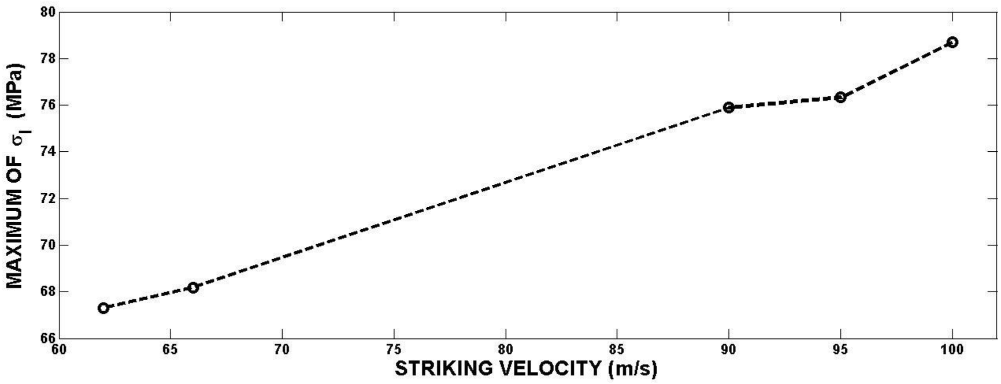

Figure 8: The maximum of the stress pulse σ_I vs. the striking velocity.

The stress pulse, $\sigma_I(t)$, may be also characterized by the following parameters:

- Impulse : $I_I = \int \sigma_I(t)\, dt$
- Energy : $w_I = \frac{1}{Z_b} \int \sigma_I^2\,(t) dt$

Each of these quantities can be expressed as a sum of two parts:

$$I_I = I_E + I_D = \int_0^{t_y} \sigma_I(\tau) d\tau + \int_{t_y}^{\lambda} \sigma_I(\tau) d\tau \qquad (5)$$

$$w_I = w_E + w_D = \frac{1}{Z_b} \int_0^{t_y} \sigma_I^2\,(\tau) d\tau + \frac{1}{Z_b} \int_{t_y}^{\lambda} \sigma_I^2\,(\tau) d\tau \qquad (6)$$

where I_E and w_E corresponds to the impulse and energy of the stress pulse up to the stress pulse maximum. t_y is the time when the stress pulse maximum is achieved. During the time up to t_y no specimen damage occurs. Its behavior is purely elastic. I_D and w_D corresponds to the part of the stress pulse when specimen damage occurs and λ denotes the stress pulse duration.

The time histories of these quantities are displayed in the Fig.9. All quantities increase with the striking velocity.

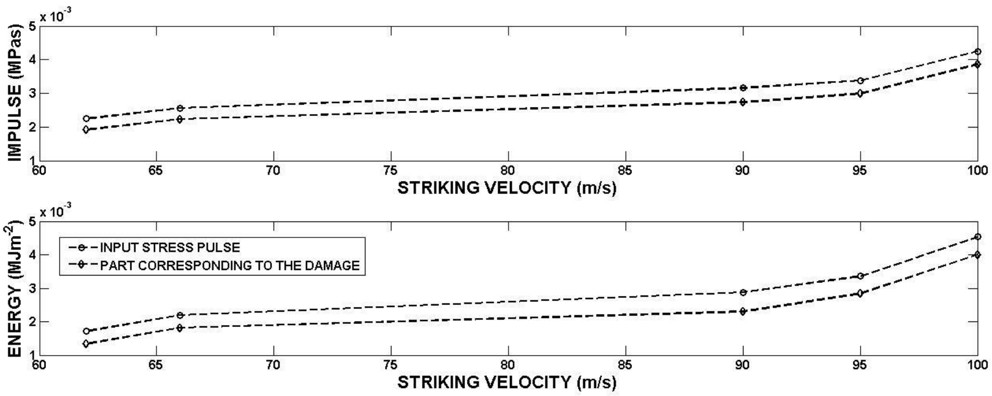

Figure 9:. The development of the stress impulse (upper part) and stress pulse energy (lower part) with the time

In the next step classical Brazilian tests – see Fig.1 were performed. The same striker was used. The impact velocities of the striker were 62, 66, 90, 95 and 100 m/s. Experimentally recorded stress pulses σ_I (t), σ_R (t), σ_T (t), are displayed in the Fig.10.

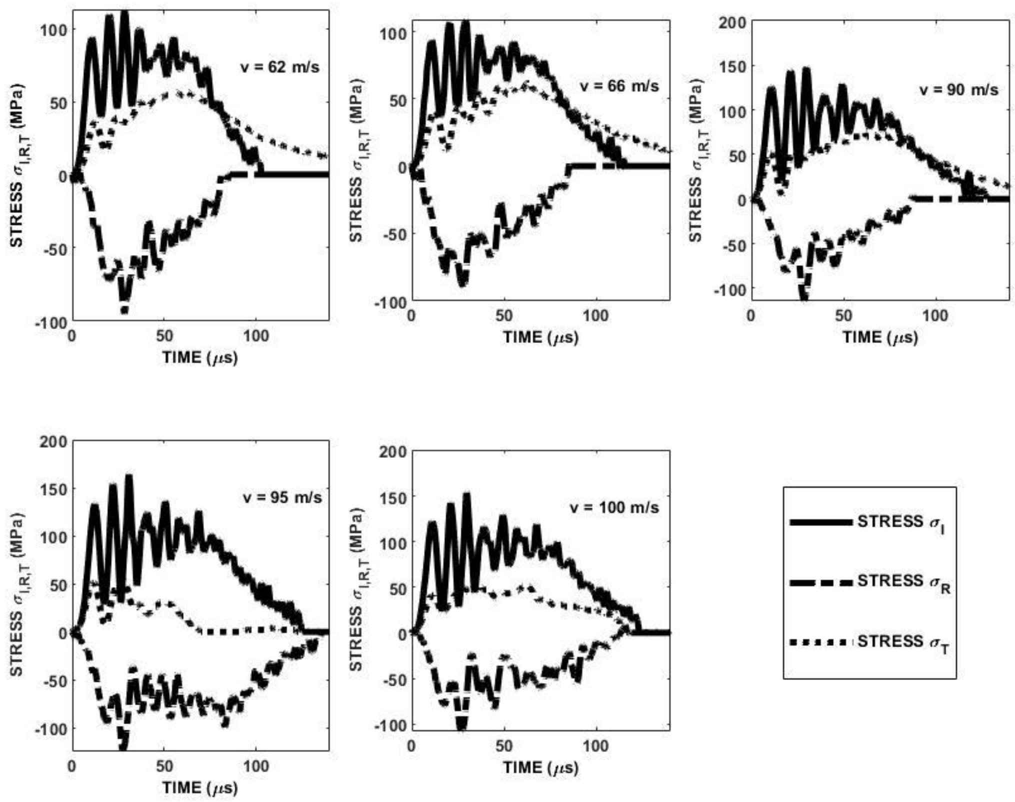

Figure 10 Experimental records of the stress pulses during the Brazilian test

Even if the input stress pulse duration is about 120 µs like e.g. in many works – see e.g. [14, 15, 18] no equilibrium in the specimen was achieved. This is documented in the Fig.11 where input stress $\sigma_I + \sigma_R$, average stress in the specimen: $\frac{1}{2}(\sigma_I + \sigma_R + \sigma_T)$ and transmitted stress σ_T are displayed.

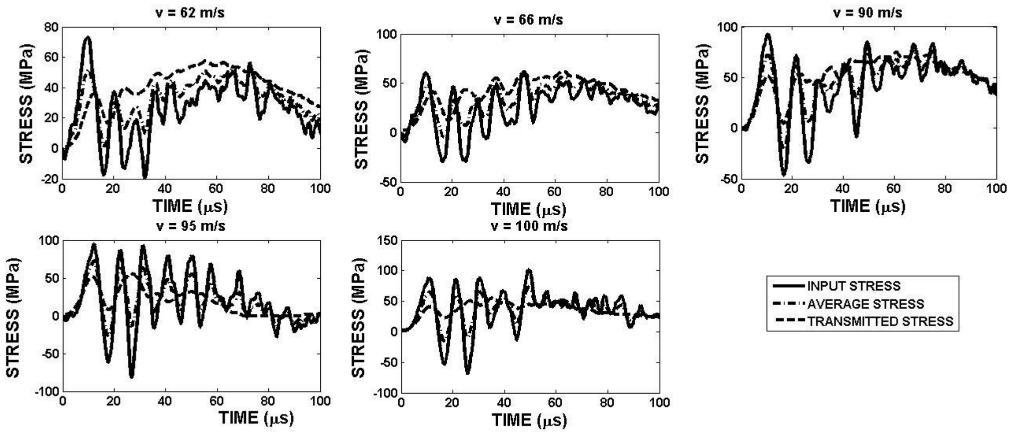

Fig.11 Input, average and transmitted stresses

The development of the specimen damage is documented in the Figs.12a-b.

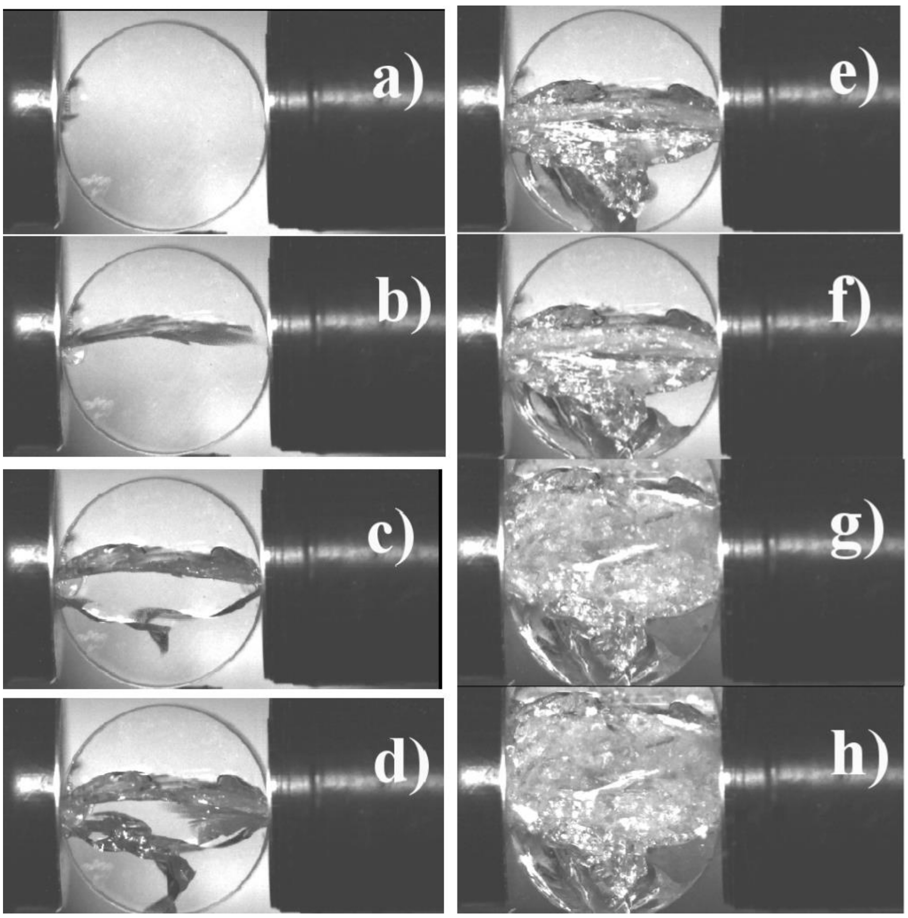

Figure 12a: High speed images of failure process in specimen at different times. Polymer striker. Striker velocity 100 m/s

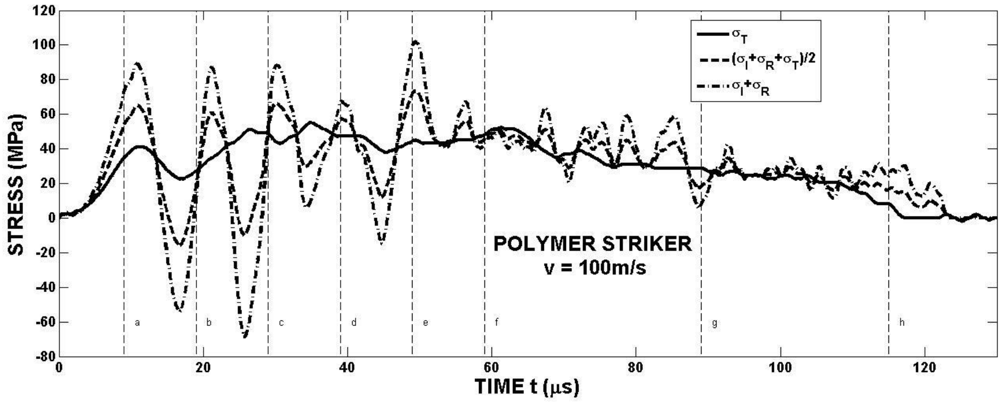

Figure 12b: Stress – time history. Position of single frames

The central cracks was developed at about 20 μs. Frames recorded at 30-60 μs show the crack bifurcation. Damage growth continues and it is followed by the specimen separation. If we compare this damage development with the record displayed in the Fig.7 (direct impact test) we can see very similar features. The same conclusions are valid for the remaining striking velocities.

Results presented in the Fig.11 show that the use of the Eq. (3) is very problematic. We have three values of the stress, input, average and transmitted. It is evident that the use of the maximum of the transmitted pulse in the Eq.(3) gives the minimum value of the tensile strength. The measure of the tensile strength at the direct impact is the maximum of the stress recorded in the Hopkinson bar. In the Fig.13 the both stresses are displayed.

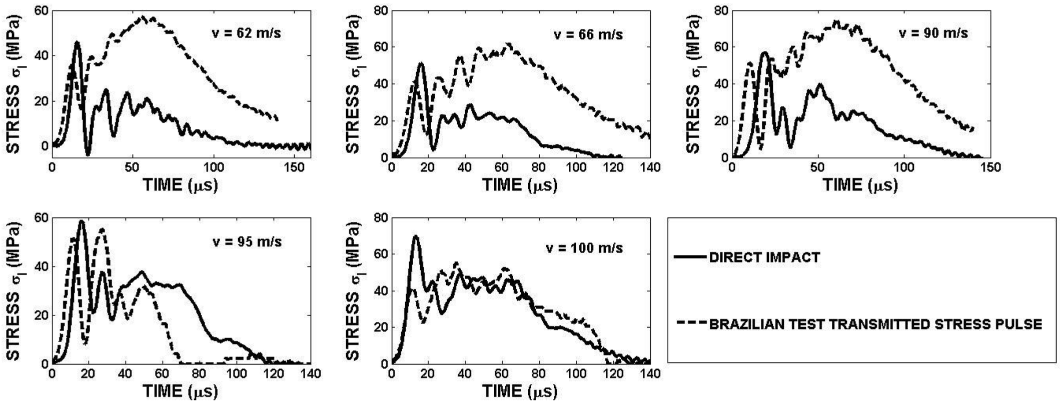

Figure 13: Transmitted stresses recorded during the direct impact and during the Brazilian test

It is obvious that the difference between time histories of the recorded pulses decreases with the increase in the striking velocity. The first peak of the stress transmitted by the specimen during the Brazilian test is lower than that reported during the direct impact test. In the Fig.14 the maxima of the input, average and transmitted stress are presented. In this the maxima of the stress recorded during the direct impact loading are also displayed.

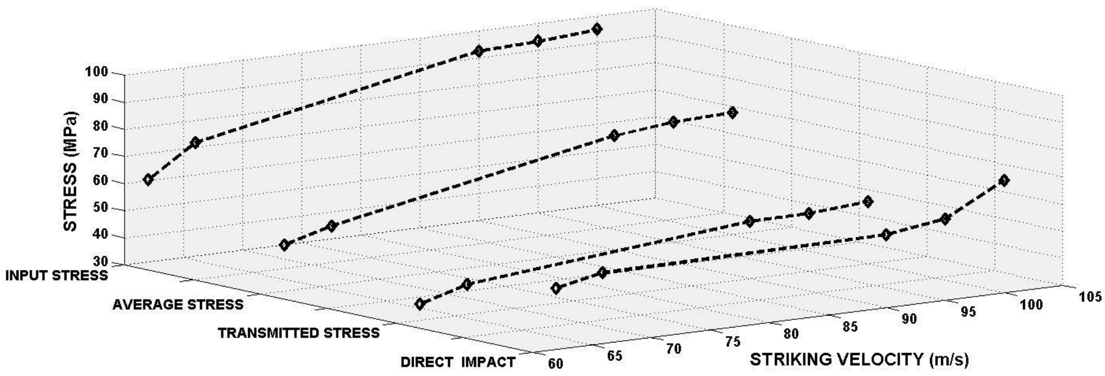

Figure 14: The values of the first peak of the stress vs. striking velocity

The value of the peak stresses increases with the increase in the striking velocity, i.e. with the increase of the specimen damage. Values of the peak stress obtained during the direct impact can be used for the comparison of different materials. Results achieved by the use of this method can be also used for the verification of different constitutive equations.

One of the most widely used constitutive models for simulating the response of glass, ceramics and other brittle materials is the JH-2 model. This constitutive equation was developed by Johnson and Holmquist [18]. Its detail description is presented e.g. in [19] where the description of its implementation in LS DYNA final element numerical code is also involved. This constitutive model incorporates the effect of damage on residual material strength and bulking during failure in compression. The relevant equations describing the response of the material are summarized in the following. The strength of the material is described by a smoothly varying function of the intact strength, fractured strength, and damage:

$$\sigma^* = \sigma_i^* - D\left(\sigma_i^* - \sigma_f^*\right) \qquad (7)$$

where stresses are normalized with respect to σ_{HEL} that is defined as

$$\sigma_{HEL} = \frac{3}{2}(HEL - P_{HEL}) \qquad (8)$$

In which, HEL is the Hugoniot elastic limit and P_{HEL} is the pressure at HEL.
The normalized intact and fractured strength are given by:

$$\sigma_i^* = A(P^* + T^*)^N(1 + Cln\dot{\varepsilon}^*)\ ,\ \sigma_f^* = B(P^*)^M(1 + Cln\dot{\varepsilon}^*) \qquad (9)$$

Where actual press P and maximum of tensile hydrostatic pressure that the material can withstand T are normalized respect to P_{HEL}.
Damage parameter D is expressed as:

$$D = \sum \frac{\Delta\varepsilon_p}{\varepsilon_p^f}$$

Where $\Delta\varepsilon_p$ is the plastic strain increment and ε_p^f is the fracture plastic strain given by:

$$\varepsilon_p^f = D_1(P^* + T^*)^{D_2}$$

The hydrostatic behaviour is described by the equation:

$$P = K_1\mu + K_2\mu^2 + K_3\mu^3 + \Delta P$$

where $\mu = \frac{\rho - \rho_0}{\rho_0}$ is the hydrostatic compression and ΔP is the bulking pressure of the material. This pressure is determined by the amount of accumulated damage. Under relatively lower pressures the only parameter K_1 can be used. In this case this parameter corresponds to the bulk modulus, which can be evaluated using common elastic constants.
The description of the brittle material using of Johnson Holmquist (JH-2) equation is based on the nine material parameters: A, B, C, M, N, T, HEL, D_1, D_2, which must be determined. The procedure of the determination of these data are described in many papers - see e.g.[20]. In this paper data taken from [21] have been used. The parameters of JH - 2 model are in the Table 3.

Table 3: Material constants for soda – lime glass

Density (kg/m^3)	2530
Strength constants	
A	0.75
B	0.2
C	0.035
N	1
M	0.72
T (MPa)	27.8
HEL (GPa)	1.003
σ_{HEL} (MPa)	334
G (GPa)	26.9
Damage constants	
D_1	0.043
D_2	0.85
Equation of state	
K_1(GPa)	43.2
K_2(GPa)	-67.2
K_3(GPa)	153.2

This model has been used in LS DYNA finite element code in order to simulate experiments shown in the Fig.2. In the Fig.15 the time history of the axial stress is displayed. It is evident that the agreement between the computed and the test results improved with the increase in the striking velocity.

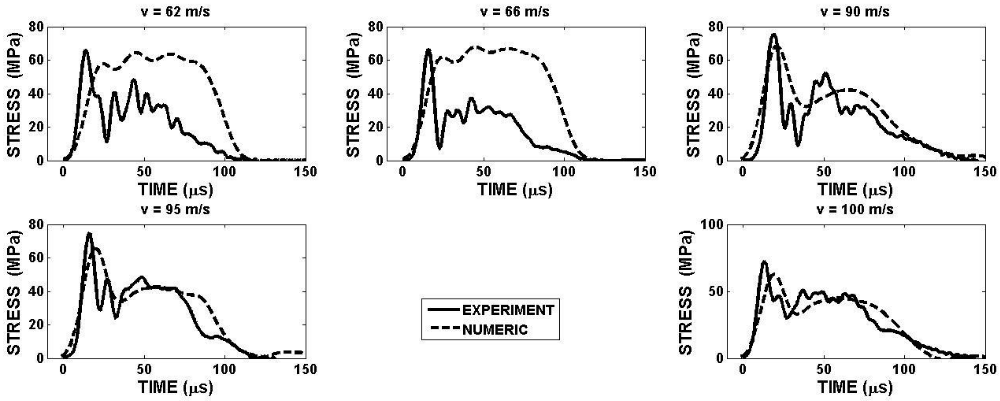

Figure 15: Comparison of the experimental and computed axial stresses for the direct impact configuration –see Fig.2

The significant difference between computed and experimental time histories of the axial stresses was reported namely at striking velocities 62 m/s (elastic response) and 66 m/s (very small specimen damage). In the next step numerical simulation of the specimen damage was evaluated. In the Fig.16 the specimen damage development at striking velocity 66 m/s is displayed. In this Figure as well in the following the striker moves from the left to right.

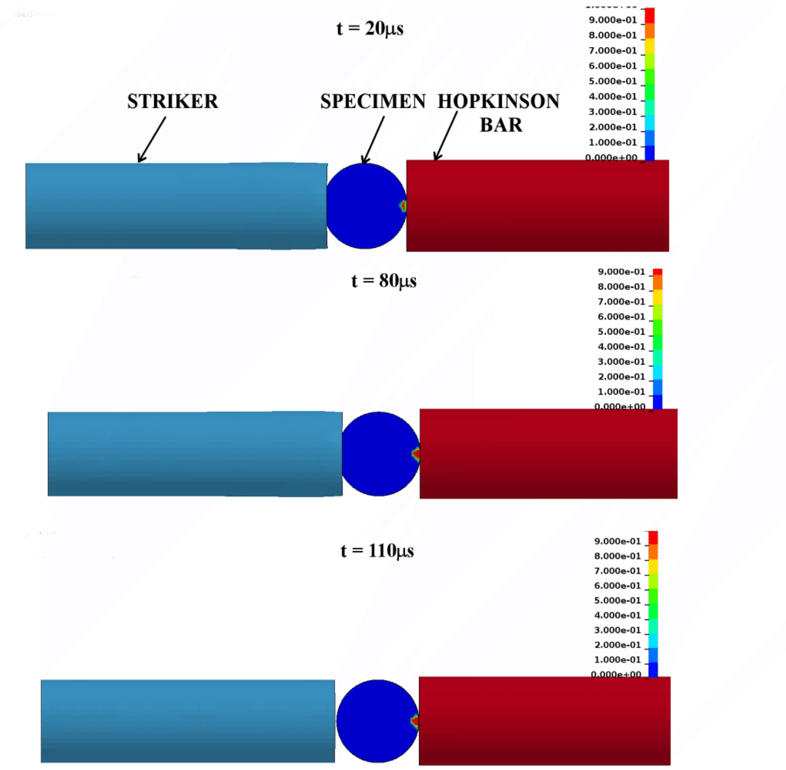

Figure 16: Numerical simulation of specimen damage development. Red color corresponds to complete damage, blue color to intact specimen. This valid also for the Figs.17 and 18.

The extent of the specimen damage is relatively small. The numerical results in the Fig.16 agree with results of experiments reported in the Fig. 4.
In the Fig.17 the damage of the specimen at the striking velocity 100 m/s is presented.

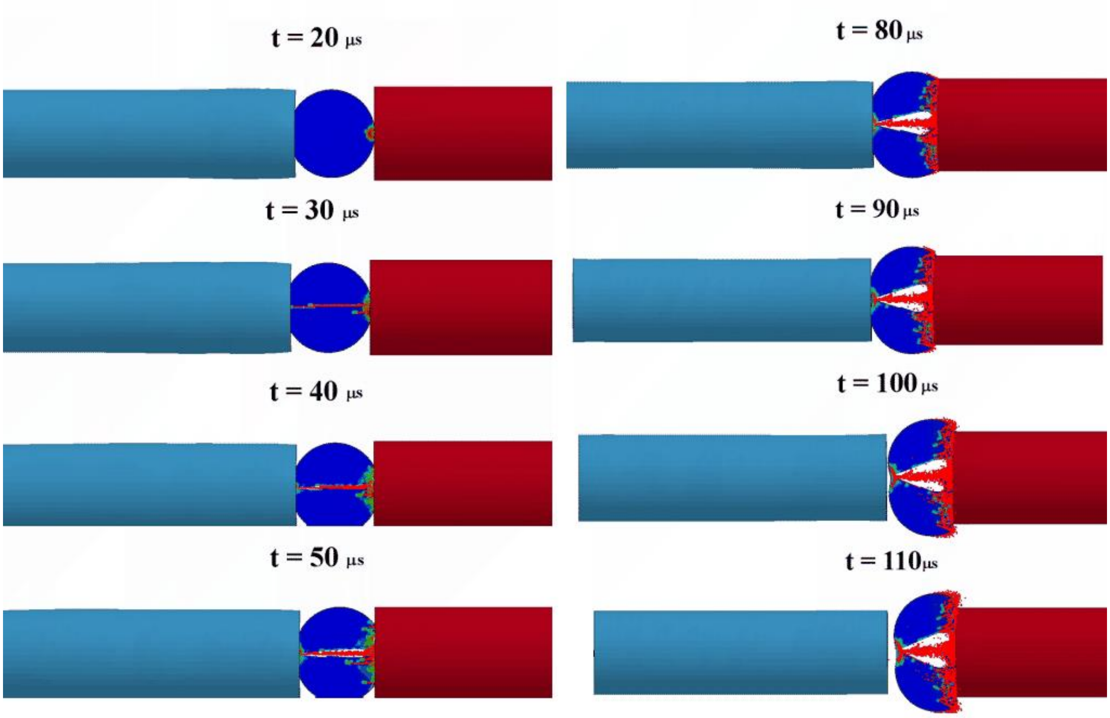

Figure 17: Numerical simulation of the specimen damage development. Striking velocity 100 m/s

The agreement between numerical and experimental results (Fig.7) may be considered up to about 30 µs. Numerical simulation of the loading process is not able to describe next specimen damage development. Numerical simulation gives similar results for the striking velocities 90, 95 and 100 m/s as it is shown in the Fig.18. In this figure the final damage of the glass specimens is shown.

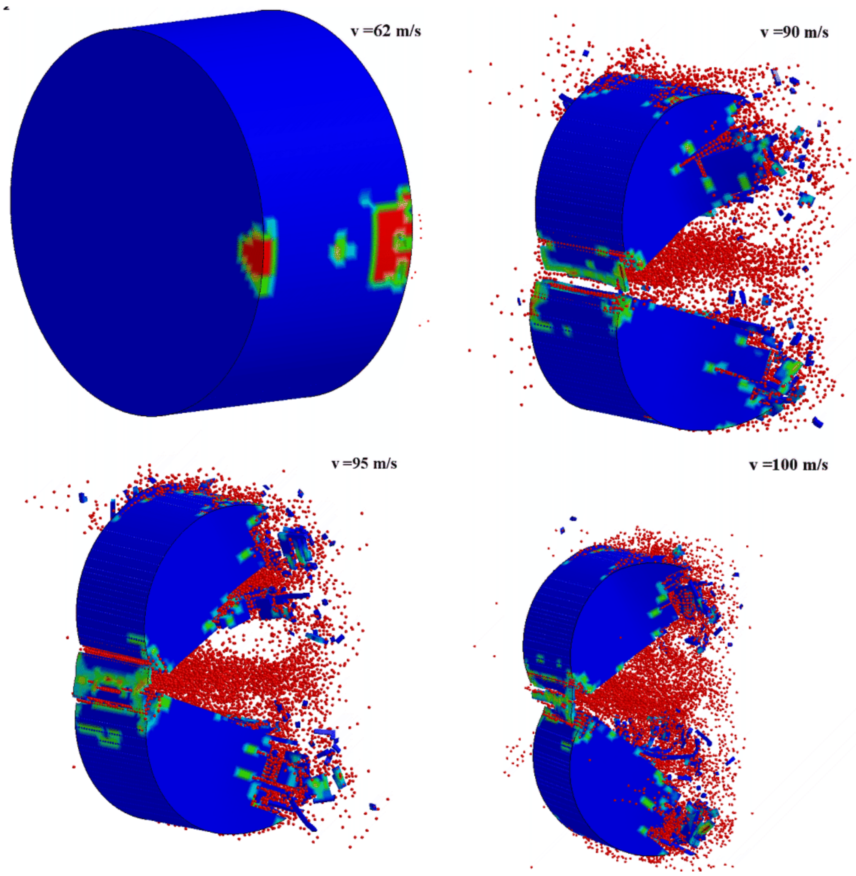

Figure 18: Final damage of the glass specimen – numerical results

IV. CONCLUSSIONS.

In the given paper the fracture of the soda – lime glass specimens under impact loading have been studied. The modified Brazilian test named as direct impact was used. These experiments show that the glass fracture resistance is well characterized by the maximum of the stress transmitted to the supporting elastic (Hopkinson) bar. This parameter increases with the projectile striking velocity. The rate dependent resistivity of tested glass to the loading rate was supported also by the results of dynamic Brazilian test. The high – speed camera results show that the main features of the specimen damage development are near the same both for the direct impact and for the Brazilian test. It means the results of the Brazilian test can be used for the prediction of the specimen fracture resistivity at direct impact loading. The preliminary results of the numerical simulation show that the agreement between numerical and experimental results depends on the striking velocity. In order to improve the computational results the material data must be obtained for the used specimens.

Acknowledgements: This research was supported by the European Regional Development Fund under Grant No. CZ.02.1.01/0.0/0.0/15_003/0000493 (Centre of Excellence for Nonlinear Dynamic Behavior of Advanced Materials in Engineering).

REFERENCES

[1]. Wei, J., Shetty, M. S., and Dharani, L. R.[2006] "Failure analysis of architectural glazing subjected to blast loading" Eng. Fail. Anal., Vol.13: pp. 1029–1043.

[2]. Kumar, P., and Shukla, A. [2011] "Dynamic response of glass panels subjected to shock loading," J. Non. Cryst. Solids, Vol. **357**: pp. 3917–3923.

[3]. Hooper, P. a., Sukhram, R. M., Blackman, B. R. K., and Dear, J. P.[2012] "On the blast Resistance of laminated glass" Int. J. Solids Struct., 49: pp. 899–918.

[4]. Larcher, M., Solomos, G., Casadei, F., and Gebbeken, N.[2012] "Experimental and numerical investigations of laminated glass subjected to blast loading" Int. J. Impact Eng., 39: pp. 42–50.

[5]. Zhang, X., Hao, H., and Ma, G.[2013] "Parametric study of laminated glass window response to blast loads" Eng. Struct., 56:pp. 1707–1717.

[6]. Hidallana-Gamage, H. D., Thambiratnam, D. P., and Perera, N. J.[2014] "Failure analysis of laminated glass panels subjected to blast loads" Eng. Fail. Anal., 36: pp. 14–29.

[7]. Sundaram, S., and Clifton, R. J.[1998] "Flow behavior of soda-lime glass at high pressures and high shear rates" The tenth American Physical Society topical conferen on shock compression of condensed matter: pp. 517–521

[8]. Flocker, F. W., and Dharani, L. R. [1997] "Stresses in laminated glass subject to low velocity impact" Eng. Struct., 19 :pp. 851–856.

[9]. Forde, L. C., Proud, W. G., Walley, S. M., Church, P. D., and Cullis, I. G.[2010] "Ballistic impact studies of a borosilicate glass" Int. J. Impact Eng., 37: pp. 568–578.

[10]. Bouzid, S., Nyoungue, a., Azari, Z., Bouaouadja, N., and Pluvinage, G.[2001] "Fracture criterion for glass under impact loading" Int. J. Impact Eng., 25: pp. 831–845.

[11]. Bourne, N. K., Forde, L. C., Millett, J. C. F., Field, J. E., Road, M., and Ohe, C. B., 1997, "Impact and Penetration of a Borosilicate Glass" **7**(1 997), pp. 1–6.

[12]. M. Peroni, G. Solomos, V. Pizzinato, M. Larcher [2011]" Experimental investigation of high strain-rate behaviour of glass" Appl. Mech. Mater. 82 :pp. 63–6.

[13]. Chocron, S., Anderson, C. E., Dannemann, K. A., and Nicholls, A. E. [2013] "Pressure Effects on the Compressive Response of Confined Intact and Damaged Soda-Lime Glass" Exp. Mech., 53: pp. 77–89.

[14]. Xihong Zhang, Yang Zou, Hong Hao, et al.[2012] " Laboratory test on dynamic material properties of annealed float glass" J. Int. Protect. Struct. 3 :pp. 407–430.

[15]. Muhammad Zakir Sheikha,Zhen Wanga, Bing Dua, Tao Suoa et al.[2019]" Static and dynamic Brazilian disk tests for mechanical characterization of annealed and chemically strengthened glass" Ceramics International ,Vol.45:pp.7931-7944.

[16]. Ferdinand P.Beer, E.Johnston, E. Russel,John Dewolf, David Mazurek.[2009] Mechanics of Materials. McGraw Hill. p. 56. ISBN 978-0-07-015389-9.

[17]. Gorfrain J.E.,Key C.T.,Alexander C.S.[2016] "Application of a Computational Glass Model to the Shock Response of Soda – Lime Glass" J.Dynamic Behaviour Mater, Vol. 2:pp. 283 – 305.

[18]. Holmquist TJ, Johnson GR [2011]"A computational constitutive model for glass subjected to large strains, high strain rates and high pressures" J Appl Mech Vol.78:051003.

[19]. Cronin D.S.,Bui K.,Kaufman Ch.,McIntosh G.,Berstadt T.[2004].Implementon and Validation of the Johnson/Holmquist Ceramic Material Model in LS-DYNA. Proceedings of the 4th European LS – DYNA Users Conference.22nd – 23rd May,Ulm,Germany.paper No D-I-48.0]. Ruggiero M.,Iannitti G.,Bonora

[20]. Ruggiero M.,Iannitti G.,Bonora M.,Ferraro M.[2012]"Determination of the Holmquist constitutive model parameters for fused silica" EPJ Web of Conferences 26:04011.

[21]. Xihong Zhang,Hong Hao, Guowei Ma [2015]" Dynamic materiál model of annealed soda – lime glas". International Journal of Impact Engineering, Vol. 77:pp.108-119.